IEEE Access
Multidisciplinary | Rapid Review | Open Access Journal

Received July 28, 2018, accepted August 23, 2018, date of publication August 29, 2018, date of current version September 21, 2018.

Digital Object Identifier 10.1109/ACCESS.2018.2867653

Study on Optimal Structure of Three-Loop Simplified Scaling Model for Dry-Type Air-Core Reactors

ZHIYUN HAN[1], LIANG ZOU[1], HAN SONG[1], LI ZHANG[1], TONG ZHAO[1], AND YOULIANG SUN[2]

[1]School of Electrical Engineering, Shandong University, Jinan 250061, China
[2]Shandong Electrical Engineering and Equipment Group Co., Ltd., Jinan 250001, China

Corresponding author: Liang Zou (zouliang@sdu.edu.cn)

This work was supported in part by the National Natural Science Foundation of China under Grant 51307102, and in part by the State Grid Corporation Key Scientific and Technological Project under Grant SGSG0000JSJS1700014.

ABSTRACT In order to predict the spatial magnetic field distribution (SMFD) of dry-type air-core reactors (DARs), the optimal structure of the three-loop simplified scaling model with adjustable ring position and turn number for DARs was investigated. First, the formulas for calculating the SMFD of the original model and the three-loop simplified model were derived according to Biot–Savart law and superposition theorem. Then, the optimal structure of the three-loop simplified model which is the closest to the original model was obtained based on the least squares method after calculating the magnetic induction intensity in six typical directions. In the typical directions, the prediction error of the optimal simplified model was less than 5.5%. Furthermore, the corresponding laws of the optimal simplified model structure in accordance with the original model structures were obtained. The results based on the magnetic field measurement platform indicate that the optimal structure of the three-loop simplified model with frequency 50 Hz is 37.5% relative height, which is very close to the structure, calculated by the corresponding law with 36.15% relative height.

INDEX TERMS Dry-type air-core reactor (DAR), spatial magnetic field distribution (SMFD), three-loop simplified scaling model, optimal structure, least squares method.

I. INTRODUCTION

Dry-type air-core reactors (DARs) have been widely utilized in power systems due to favorable linearity, low loss, stable parameters and good fire resistance [1]–[5]. In spite of this, a strong magnetic field referred to as spatial magnetic field is inevitably generated surrounding DARs when under operating condition. Since DARs are primarily manufactured using pillar supports, the influence of the axial magnetic field on the grounding grid and the radial magnetic field on the surrounding electrical equipment are both nonnegligible [6]–[11]. More seriously, under the above circumstances, eddy currents and circulation may occur in the ferromagnetic materials nearby DARs resulting in core loss increase, temperature rise and misoperation of DAR protection functions [12]–[16]. It is becoming increasingly necessary and urgent to investigate the spatial magnetic field distribution (SMFD) and magnetic field prediction for DARs.

Although the SMFD can be measured accurately and intuitively by field measurement, plenty of human and material resources should be invested before any desired results are received. Besides, no data of SMFD can be measured before the construction of DAR is finished.

Up to now, two kinds of experimental scaling models of DARs based on Similarity Theory have been proposed to predict SMFD, which are the Scaling Models and the Simplified Scaling Models. After the scaling rules are set up, magnetic field of the scaling models along any direction can be easily measured as to predict the SMFD of DARs under the design stage.

With respect to the Scaling Models, both of the electrical parameters and SMFD can be obtained from the geometric similarity expansion after deriving the similarity principles of DARs [17], [18]. However, winding a scaling model of a multi-encapsulated multi-layer DAR is still complicated and time-consuming in laboratory. It is necessary to find a simpler experimental model of DARs before they are manufactured.

The Simplified Scaling Models which are only composed by two or three loops of superimposing three coaxial coils

along the axial direction were proposed to overcome the difficulties of the Scaling Models. Yu *et al.* [19], [20] built three different simplified scaling models including the SINGLE model, 3FIXED model and FLEXIBLE model, in which magnetic flux densities were calculated along 5 typical traverses. Obviously, it is crucially important to optimize the structural parameters of simplified scaling models in order that the SMFD along the typical directions is as similar to the original DARs as possible. However, little research has focused on the optimal structure of simplified scaling models.

In this paper, the optimal structure of the simplified scaling model of DARs was investigated based on a three-loop simplified scaling model with adjustable ring position and turn number. Firstly, the mathematical expression of the original model and the simplified scaling model to calculate the SMFD in typical directions were derived according to Biot-Savart law. Then, the effects of distance between adjacent coils and turns of coils on SMFD of the simplified model were studied. The optimal structure of the simplified scaling model was obtained through simulation based on least squares method. Finally, a magnetic field measurement platform of simplified scaling model was established, whose results were statistically analyzed to demonstrate the validity of the optimal simplified scaling model.

II. THREE-LOOP SIMPLIFIED MODEL OF THE DAR

A single package DAR was selected as the original model because the structure with several parallel packages of DARs can be equivalent to a single package structure [21]. As shown in Fig. 1(a), six typical directions, referred by abbreviations ATC, ATS, ATH, LTB, LTC, and LTH, were chosen to represent the SMFD of the entire space of the DAR as follows:

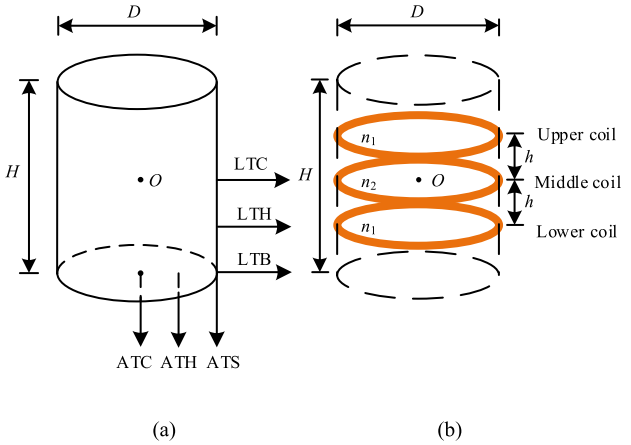

FIGURE 1. Original model and three-loop simplified scaling model of a single package DAR. (a) Original model. (b) Three-loop simplified model.

ATC: axial traverse, center,
ATS: axial traverse, side,
ATH: axial traverse, halfway between ATC and ATS,
LTB: lateral traverse, bottom,
LTC: lateral traverse, center
LTH: lateral traverse, halfway between LTB and LTC.

As shown in Fig. 1(b), a three-loop simplified scaling model of the DAR shown in Fig. 1(a) was composed by superimposing three coaxial coils along the axial direction. The upper and lower coil with n_1 turns are positioned at a distance of h on both sides of the center point O of the DAR. The middle coil is fixed in the center of the DAR whose number of turns is n_2. The total number of turns of the simplified model is $n = 2 \times n_1 + n_2$. The simplified model and original model should satisfy the principle of equal total ampere-turns for the purpose of producing the same magnetic field [20].

TABLE 1. Parameters of original model and simplified model.

Parameters	Original Model	Simplified Model
Axial Height	H	H
Basal Diameter	D	D
Line Width	W	W
Total Number of Turns	N	n
Current	I	i

TABLE 2. Parameters of simplified model.

Parameters	Symbol
Distance Between Upper (or Lower) and Middle Coil	h
Relative Height Percentage	ρ
Turns of Upper (or Lower) Coil	n_1
Turns of Middle Coil	n_2
Relative Turns Percentage	η

The variable names of the parameters of the original model and the simplified model are shown in Table 1. The ratio of height to diameter (H/D) was proposed due to different structures of DARs in power substations and plants. The parameters of the simplified model are shown in Table 2. The relative height percentage ($\rho = h/H \times 100\%$) and the relative turns percentage ($\eta = n_2/n \times 100\%$) indicate the different spatial structures of the simplified model. With regard to each different H/D corresponding to the original model, an optimal simplified model structure that best matches the SMFD of the original model can be found.

III. CALCULATION OF SMFD

As shown in Fig. 2, assuming the radius of a given current-carrying loop is R. Taking the center O of the loop as the origin, the coordinate system was established where the plane of the loop is the xOy plane, the central axis of the loop is the z-axis. The mathematical expression of the loop is as follows:

$$x^2 + y^2 = R^2 \tag{1}$$

$P(x, y, z)$ is an arbitrary point in space, and $A(x_1, y_1, 0)$ is an arbitrary point on the loop. The current element at point A

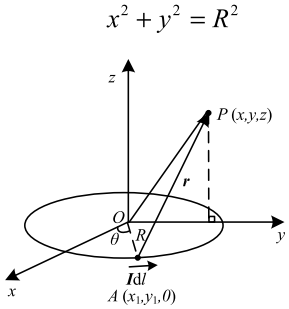

FIGURE 2. Calculation of the SMFD of the single current-carrying loop.

satisfies:

$$Id\overrightarrow{l} = IR\left(-\overrightarrow{i}\cdot\sin\theta + \overrightarrow{j}\cdot\cos\theta\right)d\theta \tag{2}$$

The position vector $\overrightarrow{r}$ of point A to point P can be expressed as:

$$\overrightarrow{r} = \overrightarrow{AP} = (x - R\cdot\cos\theta)\overrightarrow{i} + (y - R\cdot\sin\theta)\overrightarrow{j} + z\cdot\overrightarrow{k} \tag{3}$$

The expression of Biot-Savart law is:

$$d\overrightarrow{B} = \frac{\mu_0 Id\overrightarrow{l}\times\overrightarrow{r}}{4\pi r^3} \tag{4}$$

where substituting (2) and (3) into (4), the magnetic induction intensity of point P can be obtained as:

$$\overrightarrow{B} = \frac{\mu_0}{4\pi}\int\frac{Id\overrightarrow{l}\times\overrightarrow{r}}{r^3} = \frac{\mu_0 IR}{4\pi}\int\frac{z\cos\theta\overrightarrow{i} + z\sin\theta\overrightarrow{j} + (R - x\cos\theta - y\sin\theta)\overrightarrow{k}}{r^3}d\theta \tag{5}$$

where in (5), $r = \left(x^2 + y^2 + z^2 + R^2 - 2xR\cos\theta - 2yR\sin\theta\right)^{\frac{1}{2}}$.

The component of the magnetic induction intensity produced by the current-carrying loop in the space can be obtained as:

$$\begin{cases}\overrightarrow{B_x} = \dfrac{\mu_0 IR}{4\pi}\displaystyle\int_0^{2\pi}\frac{z\cos\theta}{r^3}\overrightarrow{i}\,d\theta\\ \overrightarrow{B_y} = \dfrac{\mu_0 IR}{4\pi}\displaystyle\int_0^{2\pi}\frac{z\sin\theta}{r^3}\overrightarrow{j}\,d\theta\\ \overrightarrow{B_z} = \dfrac{\mu_0 IR}{4\pi}\displaystyle\int_0^{2\pi}\frac{R - x\cos\theta - y\sin\theta}{r^3}\overrightarrow{k}\,d\theta\end{cases} \tag{6}$$

A. SMFD OF ORIGINAL MODEL

Taking the bottom plane of the original model as the xOy plane, the space rectangular coordinate system was established where the axis of the original model is the z-axis, the center O of the bottom plane is the origin. Neglecting the influence of the winding pitch angle, the SMFD of the original model can be obtained according to the superposition theorem. The magnetic induction intensity of a point $P(x, y, z)$ in space is as follows:

$$\begin{cases}\overrightarrow{B_x} = \displaystyle\sum_{l=0}^{N-1}\frac{\mu_0 IR}{4\pi}\int_0^{2\pi}\frac{(z - lW)\cos\theta}{r^3}\overrightarrow{i}\,d\theta\\ \overrightarrow{B_y} = \displaystyle\sum_{l=0}^{N-1}\frac{\mu_0 IR}{4\pi}\int_0^{2\pi}\frac{(z - lW)\sin\theta}{r^3}\overrightarrow{j}\,d\theta\\ \overrightarrow{B_z} = \displaystyle\sum_{l=0}^{N-1}\frac{\mu_0 IR}{4\pi}\int_0^{2\pi}\frac{R - x\cos\theta - y\sin\theta}{r^3}\overrightarrow{k}\,d\theta\end{cases} \tag{7}$$

where in (7), $r = \left(\left(x - R\cos\theta\right)^2 + (y - R\sin\theta)^2 + (z - lW)^2\right)^{\frac{1}{2}}$.

B. SMFD OF THREE-LOOP SIMPLIFIED MODEL

The coordinate systems of the three-loop simplified model are the same as the original model. The simplified model of the DAR was established by superimposing three coaxial coils in the axial direction. The line width of the coaxial coil is W, and the current in the wire is i. The turns of the three coils are $\boldsymbol{n}$=[n_1, n_2, n_1], and the positions are $\boldsymbol{h}$=[$H/2 - h$, $H/2$, $H/2+h$]. Neglecting the influence of the winding pitch angle, the SMFD of the simplified model can be obtained according to the superposition theorem. The magnetic induction intensity of a point $P(x, y, z)$ in space is as follows:

$$\begin{cases}\overrightarrow{B_x} = \displaystyle\sum_{l=1}^{3}\frac{\mu_0 iR\cdot\boldsymbol{n}(l)}{4\pi}\int_0^{2\pi}\frac{(z - \boldsymbol{h}(l))\cos\theta}{r^3}\overrightarrow{i}\,d\theta\\ \overrightarrow{B_y} = \displaystyle\sum_{l=1}^{3}\frac{\mu_0 iR\cdot\boldsymbol{n}(l)}{4\pi}\int_0^{2\pi}\frac{(z - \boldsymbol{h}(l))\sin\theta}{r^3}\overrightarrow{j}\,d\theta\\ \overrightarrow{B_z} = \displaystyle\sum_{l=1}^{3}\frac{\mu_0 iR\cdot\boldsymbol{n}(l)}{4\pi}\int_0^{2\pi}\frac{R - x\cos\theta - y\sin\theta}{r^3}\overrightarrow{k}\,d\theta\end{cases} \tag{8}$$

where in (8), $r = \left((x - R\cos\theta)^2 + (y - R\sin\theta)^2 + (z - \boldsymbol{h}(l))^2\right)^{\frac{1}{2}}$.

IV. SIMULATION OF OPTIMAL STRUCTURE THREE-LOOP SIMPLIFIED MODEL

The DAR models with H/D value from 0.5 to 2 were investigated where the fixed bottom diameter is selected as $D = 124$ mm and the wire width as $W = 0.6$ mm. The current of the original model coil is $I = 1.5$ A and the frequency $f = 50$Hz. The height is selected as 0.5-2 D, that is, 62-248 mm. The original model is considered to be tight winding, and the number of turns is selected as 104-414. To facilitate the calculation, a total of 31 sets of models were selected as the object of study, with 100-400 turns and an interval of 10. The current of the simplified model coil was calculated according to the principle of equal total ampere-turns, i.e., $i = NI/n$. In order to make the ring of the simplified model have the right size, the total turns of the simplified model are set to 3/5 of the turns of the original model, i.e., $n = 3N/5$. The wire width, the bottom diameter and the height of the simplified model are all consistent with

the original model. The contribution of the eddy current, skin effect, and background magnetic field are neglected.

A. INFLUENCE OF h ON SMFD

First, the influence of h changes of three-loop simplified model on SMFD was discussed so as to obtain the relationship between the coil height and optimal simplified structure. The number of turns of the three coils is equal to each other.

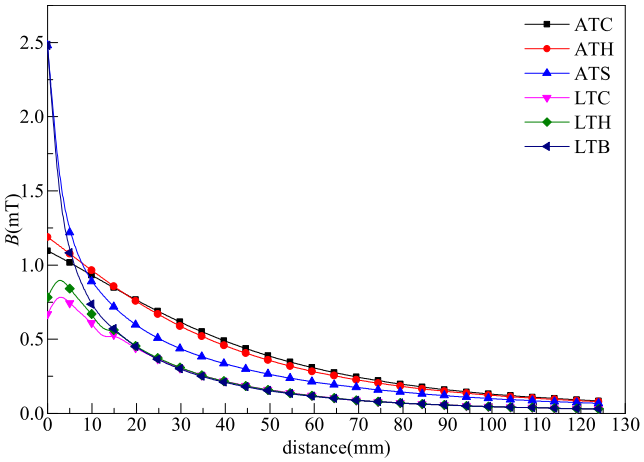

FIGURE 3. Magnetic induction intensity in the six typical directions of the original model.

The magnetic induction intensity in the six typical directions of the original model of $N = 100$ is shown in Fig. 3. The ATC curve is similar to the ATH curve, while the LTC curve is similar to the LTH curve. As the measurement point moves away from the reactor, the magnetic induction intensity decreases to be consistent gradually, which means ATC and ATS, LTC and LTB can represent all directions between these two directions, respectively. Due to the longitudinal symmetry and cylindrical symmetry of DARs, the four directions, ATC, ATS, LTC, and LTB, can represent all the spatial directions of the reactor model.

The least squares method was utilized to find the optimal simplified model structure which was obtained by minimizing the magnetic induction intensity square error sum at each point in space. For a point $P(x, y, z)$ in space, the error of magnetic induction intensity is as follows:

$$e = |B_o| - |B_s| \tag{9}$$

where $|B_o|$ is the module value of the original model magnetic induction intensity, $|B_s|$ is the model value of the simplified model magnetic induction intensity.

Using the ATC direction as an example, 50 equal interval points were selected on a line segment from point (0, 0, 0) to point (0, 0, $-D$). The magnetic induction intensity error of each point was calculated. The square loss function is obtained as follows:

$$Q_{ATC} = \sum_{i=1}^{n} e_i^2, \quad n = 50 \tag{10}$$

The optimal simplified model in the ATC direction can be obtained by searching for the smallest Q_{ATC}. To find the overall optimal structure, the minimum value of the sum of Q values in the four directions should be found. The constraint is as follows:

$$Q_{\min} = Q_{ATC} + Q_{ATS} + Q_{LTC} + Q_{LTB} \tag{11}$$

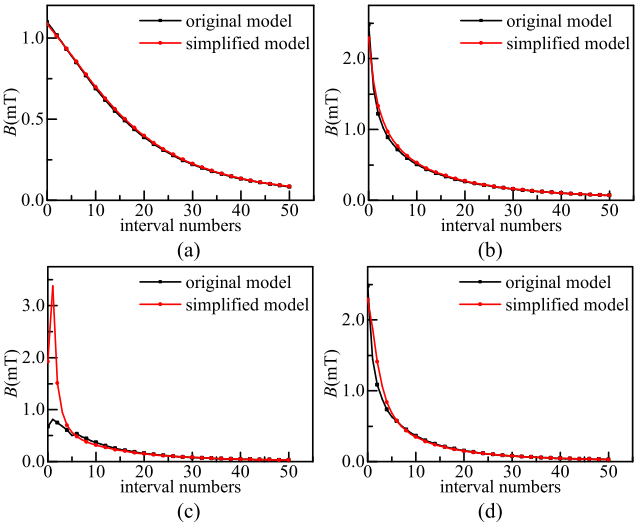

FIGURE 4. Magnetic induction intensity of the original model and the ρ=41% three-loop simplified model in four typical directions. (a) ATC direction. (b) ATS direction. (c) LTC direction. (d) LTB direction.

When $N = 100$, $Q_{\min} = 9.3 \times 10^{-6}$ can be calculated. The structure of the optimal simplified model is $\rho = 41\%$. As shown in Fig. 4, the SMFD of the simplified model in the ATC, ATS and LTB directions is a good substitute for the original model when $\rho = 41\%$. However, the SMFD of the simplified model along the LTC direction in the near-field region is distinctly different from the SMFD in the original model. The difference of the structure between the original model and the simplified model results in the difference of the SMFD. The original model is a coaxial solenoid, in which the magnetic field mainly concentrates on the axial direction and the magnetic induction intensity in the LTC near-field region is very small. The magnetic flux leakage of the middle coil of the simplified model near the LTC near-field region leads to a relatively large magnetic induction intensity.

The range of the near field is found to increase as the height of the original model increases. The range of the near field can be obtained as 0-H/5 via several calculations. Considering that the electrical equipment is not installed in the near-field region of the actual DAR, the SMFD in the LTC direction is studied in the range of H/5-D.

Fig. 5(a) shows a positive correlation between h in the optimal simplified model and H in the original model. As shown in Fig. 5(b), ρ in the optimal simplified model decreases as H/D in the original model increases. This relationship can be expressed by the fitting formula as follows:

$$\rho(\%) = 39.3554 - 4.2786 \times (H/D) + 1.3343 \times (H/D)^2 \tag{12}$$

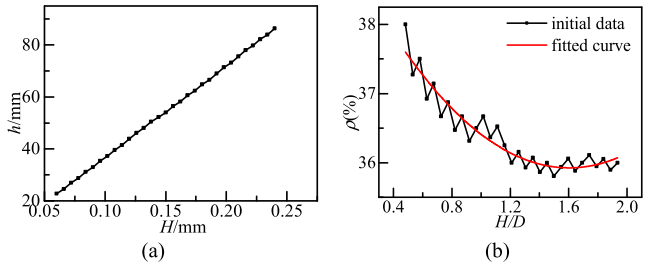

FIGURE 5. Relationship between optimal simplified model structure and original model structure. (a) Relationship between *h* and *H*. (b) Relationship between ρ and *H/D*.

The residual sum of squares (RSS) of (12) is 0.829004, and the adjusted R-square is 0.898855. These parameters show that the fitting formula has a satisfactory effect.

The root mean square error (RMSE) is defined as follows:

$$\mathrm{RMSE} = \sqrt{\frac{1}{n}\sum_{i=1}^{n}(y_i - f_i)^2} \tag{13}$$

where y_i is the actual value and f_i is the predictive value. The RMSE was utilized as a criterion for simplified model prediction accuracy. The smaller the RMSE, the higher the prediction accuracy. As shown in Fig. 6(a), the RMSE of the optimal model increases as the H/D of the original model increases. This correlation shows that the prediction effect of the optimal model gradually decreases as the original model H/D increases. With increasing H/D, the relation among the three coils of the simplified model becomes weaker and the magnetic flux leakage in each coil increases. The RMSE of the optimal simplified model is in the range of 0.026-0.045 mT when the value of H/D is in the range of 0.5-2.

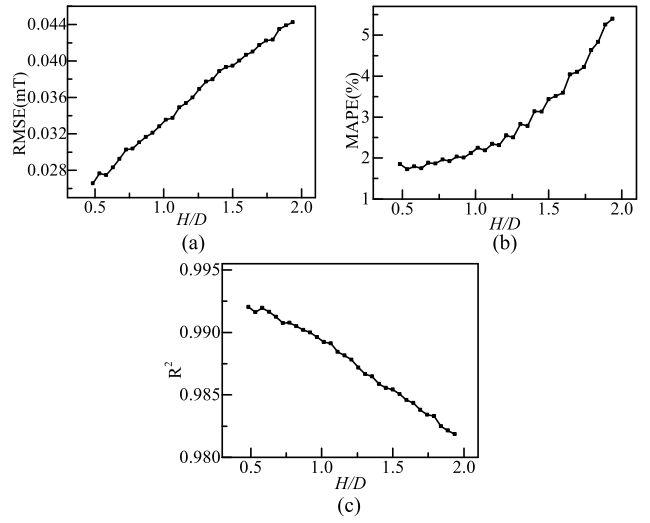

FIGURE 6. RMSE, MAPE and R^2 as a function of *H/D*. (a) RMSE. (b) MAPE. (c) R^2.

The mean absolute percentage error (MAPE) is defined as follows:

$$\mathrm{MAPE} = \frac{100}{n}\sum_{i=1}^{n}\left|\frac{y_i - f_i}{y_i}\right| \tag{14}$$

where y_i is the actual value, and f_i is the predictive value. The MAPE is a measurement statistic that describes the accuracy of prediction methods. As shown in Fig. 6(b), the MAPE of the optimal model increases as H/D increases. The changing trend of the MAPE is consistent with that of the RMSE. The MAPE of the optimal simplified model is in the range of 1.5-5.5% when the value of H/D is in the range of 0.5-2. This correlation shows that the optimal three-loop simplified model has satisfactory prediction accuracy.

The determination coefficient (R^2) is a quantitative index indicating the intimate level of correlation between the predicted value and actual value, as shown in (15).

$$R^2 = 1 - \frac{SS_{res}}{SS_{tot}} \tag{15}$$

where total sum of squares $SS_{tot} = \sum_{i}^{n}(y_i - \bar{y})^2$, residual sum of squares $SS_{res} = \sum_{i}^{n}(y_i - f_i)^2$, and the mean value of actual value $\bar{y} = \frac{1}{n}\sum_{i}^{n} y_i$.

As shown in Fig. 6(c), the R^2 of the optimal model decreases as H/D increases. However, the R^2 remains above 0.98, which ensures the accuracy of the predicted magnetic field of the simplified model.

B. INFLUENCE OF h AND n_2 ON SMFD

In the simulation, the turn number of the three-loop middle coil (n_2) is in the range from 1 to $(n-2)$. The turn number of the remaining two coils is $n_1 = (n - n_2)/2$. Fig. 7(a) shows the relationship between h of the optimal model and H of the original model when n_2 varies. Taking n_2 as the z-axis, different colors indicate different values of n_2. The relationship between h and H is consistent when n_2 varies, while h increases as H increases. The line connected by black dots in Fig. 7(a) is a curve formed by connecting points of $n_2 = n/3$. The projection of the line on the H-h plane is the graph in Fig. 5(a). Furthermore, the structure of the optimal model corresponding to each original model can be

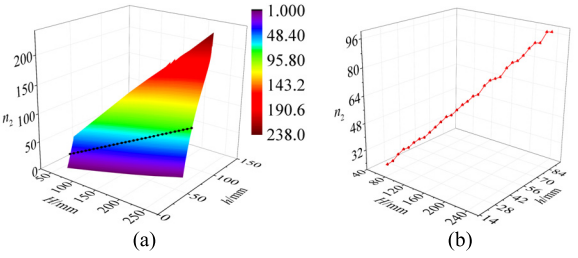

FIGURE 7. (a) Relationship between h and *H* as n_2 varies. (b) Relationship between (h, n_2) and *H*.

obtained, and the structure parameter (h, n_2) of the optimal model is uniquely determined. Fig. 7(b) shows the relationship between the structure parameter (h, n_2) of the optimal model and H of the original model. The structure parameter (h, n_2) increases as H increases where significantly positive correlation exists.

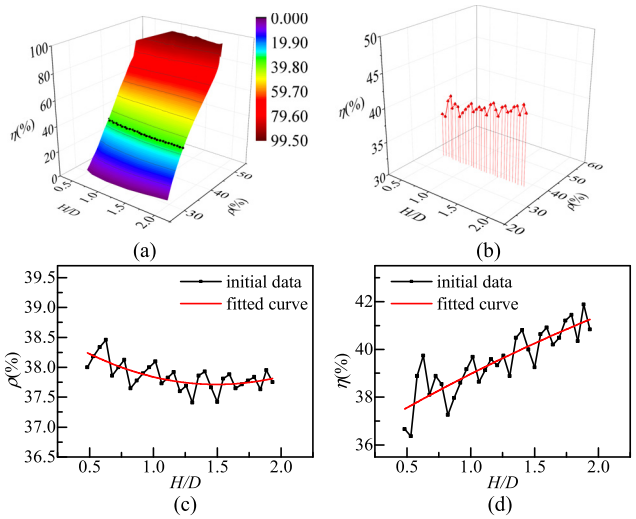

FIGURE 8. (a) Relationship between ρ and H/D as η varies. (b) Relationship between (ρ, η) and H/D. (c) Relationship between ρ and H/D. (d) Relationship between η and H/D.

Fig. 8(a) shows the relationship between ρ of the optimal simplified model and H/D of the original model when $\eta = n_2/n \times 100\%$ varies. The relationship between ρ and H/D is consistent as η varies. At the same time, there is a positive correlation between $\rho$and η when H/D is determined, because the magnetic field produced by the middle coil of the simplified model becomes stronger as the number of turns of the middle coil increases. The magnetic field produced by the remaining two coils which should be far from the middle coil becomes weak. In Fig. 8(a), the line connected by black dots represents the relationship between ρ and H/D when η is 33%. The projection of the line on the H/D-ρ plane is shown in Fig. 5(b). As shown in Fig. 8(b), the structure of the optimal model corresponding to each original model can be obtained, and the structure parameter (ρ, η) of the optimal model is unique. As can be seen from Fig. 8(c) and 8(d), the ρ of the optimal model decreases as H/D increases, and the η of the optimal model increases as H/D increases. The relationship between them can be expressed by the fitting formula as follows:

$$\begin{cases} \rho(\%) = 38.870 - 1.548 \times (H/D) + 0.518 \times (H/D)^2 \\ \eta(\%) = 36.012 + 3.220 \times (H/D) - 0.265 \times (H/D)^2 \end{cases} \tag{16}$$

As shown in Fig. 9(a), the RMSE increases as H/D increases. The RMSE of the optimal model is in the range from 0.025 to 0.043 mT when the value of H/D is in the range from 0.5 to 2. The RMSE of the optimal model is

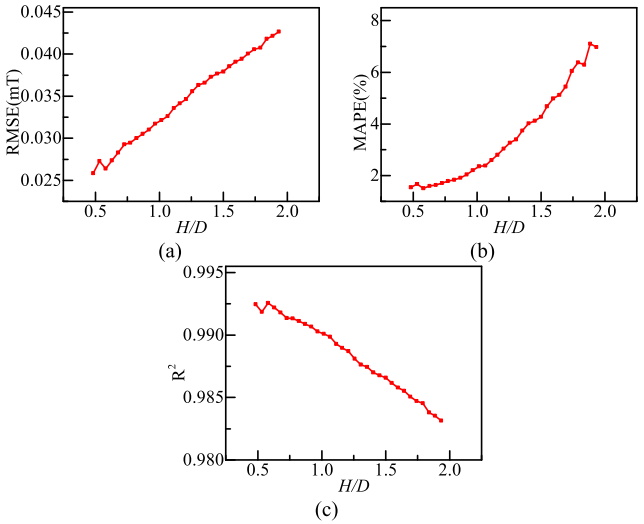

FIGURE 9. RMSE, MAPE and R^2 as a function of H/D. (a) RMSE. (b) MAPE. (c) R^2.

less than that of the model discussed in the previous section, in which only h is taken into account. This correlation shows that the prediction error is obviously smaller when h and n_2 change simultaneously. As shown in Fig. 9(b), the MAPE increases as H/D increases. Moreover, the growth rate of MAPE is faster and the prediction effect of the optimal simplified model becomes worse as H/D increases. However, the MAPE of the optimal model is in the range from 1% to 7% when the value of H/D is in the range from 0.5 to 2. The MAPE in the ATC direction is less than 2%, which is a satisfactory accuracy in engineering applications. As shown in Fig. 9(c), the R^2 of the optimal model decreases as H/D increases. R^2 also reflects that the prediction error increases as H/D increases. However, the R^2 remains above 0.98 which ensures the accuracy of the predicted magnetic field of the simplified model.

V. EXPERIMENT

A magnetic field measurement platform of DAR was built in the laboratory. As shown in Fig. 10(a), the original model is

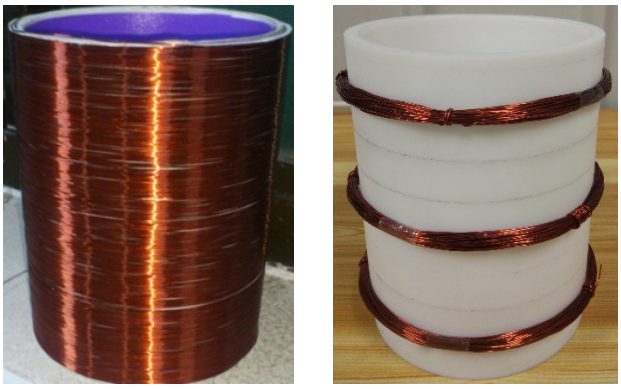

FIGURE 10. Original model and simplified model of a single package DAR. (a) Original model. (b) Simplified model.

tightly wrapped with copper enameled wire whose height is 148 mm, i.e., $H/D = 1.19$. Other parameters of the original model are the same as those in Section IV. To facilitate the experiment, a three-loop simplified model consisting of three coils with equal turns was built, as shown in Fig. 10(b), with the coil height h of the simplified model set to $H/8$, $H/4$, $3H/8$ and $H/2$.

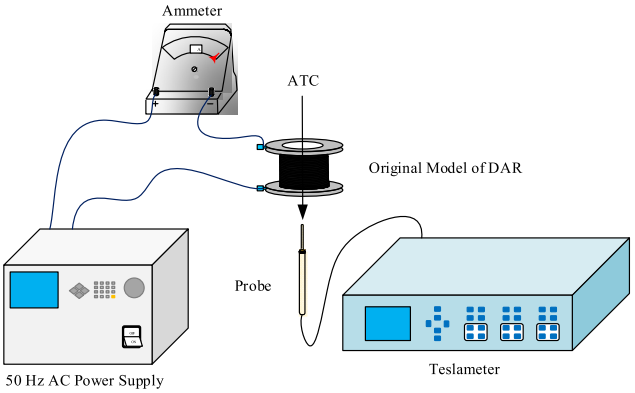

FIGURE 11. Schematic diagram of the magnetic field measurement in the ATC direction of the original model.

The schematic diagram of the magnetic field measurement of the original model is shown in Fig. 11. An AC power with frequency $f = 50$Hz supplies the required current of the original model. The ammeter is used to measure the current in the circuit. The teslameter with a resolution of 0.01μT is used to measure the magnetic induction intensity, and the magnetic induction intensity of the background magnetic field is 0.03 μT. The measurement error of the magnetic induction intensity in the LTC direction is large due to its small magnetic induction intensity. The two curves of the magnetic induction intensity in the ATS and LTB directions are similar which can be used to represent the entire spatial SMFD of the reactor.

The SMFD of the four simplified models and the original model in the ATC and LTB directions were repeatedly measured 10 times, and the mean and standard deviation of these 10 data sets were obtained. Fig. 12 shows the SMFD measurement results of the four simplified models and the original model. As can be seen from Fig. 12(a) and 12(b), the SMFD curve of the $3H/8$ simplified model is most similar to that of the original model in both ATC and LTB directions.

The statistical parameters of the four simplified models are shown in Table 3. According to (12), when $H/D = 1.19$, the structure of the optimal model is $\rho = 36.15\%$. The RMSE of the $3H/8$ simplified model is only 0.0340 mT, which is the smallest compared with the rest of the simplified models. Analogously, the MAPE of the $3H/8$ simplified model is also the smallest, with a value of 7.31%. The MAPE of the $3H/8$ simplified model has not been reduced to a minimum of 2.5% because the difference of structure between the $3H/8$ simplified model and the optimal model is still 1.35%. Comparing the SMFD of the four simplified models, it is revealed that

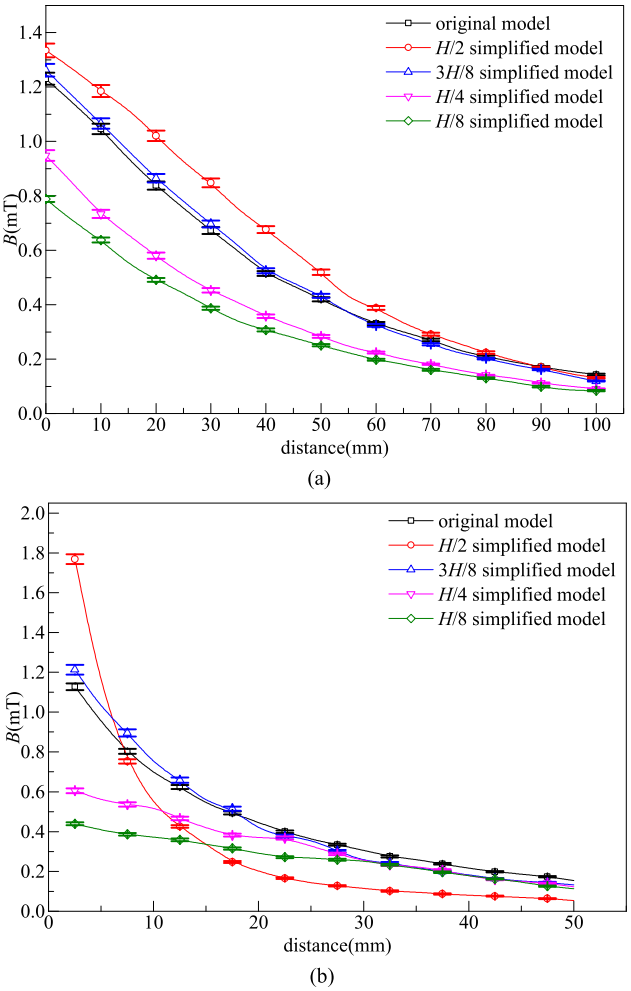

FIGURE 12. SMFD measurement results of the four simplified models and the original model in two directions. (a) ATC direction. (b) LTB direction.

TABLE 3. Statistical parameters of the four simplified models.

h	$H/2$	$3H/8$	$H/4$	$H/8$
RMSE	0.1749 mT	0.0340 mT	0.1774 mT	0.2487 mT
MAPE	32.74%	7.31%	26.45%	36.93%

both the RMSE and MAPE of the $3H/8$ simplified model are the minimums. The SMFD of the $3H/8$ simplified model in the ATC and LTB directions is closest to the original model. Therefore, the $3H/8$ simplified model is considered to be the optimal model in the experiment, whose structure $\rho = 37.5\%$ is very close to the structure $\rho = 36.15\%$ of the optimal model obtained by simulation. The results prove the correctness of the simulation conclusion.

VI. CONCLUSIONS

According to the current research on DARs, a three-loop simplified model of a DAR was proposed. The structure of the simplified model is optimized by comparing the SMFD

in several typical directions. The results of the simulation and the experiment are showed as follows:

In the LTC direction, the SMFD of the simplified model in the near-field region is less than that of the original model. This difference arises because of magnetic flux leakage around the three coils. In the calculation of the optimal simplified model structure, it is necessary to remove the near-field region in the LTC direction.

When the number of turns of the three coils is equal, the ρ of the optimal simplified model decreases as the H/D of the original model increases. The relationship between ρ and H/D can be expressed by the fitting formula (12). As H/D increases in the original model, the RMSE of the optimal model increases gradually, MAPE increases, and R^2 decreases. The prediction error of the optimal model increases as H/D increases. When the value of H/D is in the range of 0.5 and 2, the RMSE of the optimal simplified model is in the range of 0.026 and 0.045 mT, MAPE is in the range of 1.5% and 5.5%, and R^2 remains above 0.98, all of which ensure the accuracy of the predicted magnetic field of the simplified model.

When the coil height and number of turns of the simplified model change simultaneously, the ρ of the optimal model decreases as H/D increases, and the η of the optimal model increases as H/D increases. The relationship between (ρ, η) and H/D can be expressed by the fitting formula (16). The three variation trends of RMSE, MAPE and R^2 are the same as those of the simplified model with three coils of equal turns. When the value of H/D is in the range of 0.5 and 2, the RMSE of the optimal simplified model is in the range of 0.025 and 0.043 mT, the MAPE is in the range of 1 and 7%, and the MAPE in the ATC direction is less than 2%. R^2 remains above 0.98, all of which ensure the accuracy of the predicted magnetic field of the simplified model.

The SMFD of the four typical simplified models with the coil height h of the simplified model set to $H/8$, $H/4$, $3H/8$ and $H/2$ was measured based on the experimental platform. The results show that both the RMSE and MAPE of the $3H/8$ simplified model are the minimum values. The SMFD of the $3H/8$ simplified model in the ATC and LTB directions is closest to the original model. According to the fitting formula (12), the structure of the optimal model is $\rho = 36.15\%$, which is very close to the structure $\rho = 37.5\%$ of the $3H/8$ simplified model, proving the accuracy of the simulation conclusion.

The three-loop simplified scaling model of DARs has potentials of magnetic field prediction with high accuracy under design stage, which is of great engineering value. In addition, as a reference for other engineering fields, the optimal model after simplification can be employed to calculate the SMFD of equipment with divergent magnetic field.

Our future studies will focus on scaling rules setup of multi-DARs considering coupling effect, and magnetic shielding effectiveness of multi-simplified scaling models.

REFERENCES

[1] Y. Wang *et al.*, "Theoretical and experimental evaluation of the temperature distribution in a dry type air core smoothing reactor of HVDC station," *Energies*, vol. 10, no. 5, pp. 623–635, May 2017.

[2] Q. D. Wang *et al.*, "The power frequency magnetic field distribution around dry-type air-core reactor," (in Chinese), *Trans. China Electrotech. Soc.*, vol. 24, no. 1, pp. 8–13, Jan. 2009.

[3] Q. Yu and S. A. Sebo, "Accurate evaluation of the magnetic field strength of large substation air-core reactor coils," *IEEE Trans. Power Del.*, vol. 13, no. 4, pp. 1114–1119, Oct. 1998.

[4] Y. Zhang *et al.*, "Research of the power frequency magnetic fields distribution around dry-type air-core reactor," in *Proc. World Automat. Congr.*, Honolulu, HI, USA, Sep./Oct. 2008, pp. 1–4.

[5] T. Sun and B. Wan, "Measurement of the electric-magnetic environment for 500 kv substation," (in Chinese), *High Voltage Eng.*, vol. 32, no. 3, pp. 51–55, Jun. 2006.

[6] D. Lin, P. Zhou, W. N. Fu, Z. Badics, and Z. J. Cendes, "A dynamic core loss model for soft ferromagnetic and power ferrite materials in transient finite element analysis," *IEEE Trans. Magn.*, vol. 40, no. 2, pp. 1318–1321, Mar. 2004.

[7] C. M. Arturi and M. Ubaldini, "Finite element analysis and calculation of the magnetic field distribution in smoothing inductors for electric traction," *IEEE Trans. Magn.*, vol. 25, no. 4, pp. 2864–2866, Jul. 1989.

[8] R. D. Cook, D. S. Malkus, M. E. Plesha, and R. J. Witt, *Concepts and Applications of Finite Element Analysis*, vol. 5, 4th ed. Hoboken, NJ, USA: Wiley, 2007, ch. 1, pp. 11–18.

[9] Z. P. Xia, Z. Q. Zhu, and D. Howe, "Analytical magnetic field analysis of Halbach magnetized permanent-magnet machines," *IEEE Trans. Magn.*, vol. 40, no. 4, pp. 1864–1872, Jul. 2004.

[10] M. A. O. Qiwu and Z. E. N. G. Qinggan, "Measurement and analysis of power frequency magnetic of air-core and iron-core reactors field," (in Chinese), *High Voltage Eng.*, vol. 29, no. 4, pp. 49–50, Apr. 2003.

[11] C. Q. Chen *et al.*, "Study and measurement on the influence of magnetic field of dry-type air core reactor on adjacent metal loop and communication apparatus," (in Chinese), *High Voltage Eng.*, vol. 27, no. 3, pp. 19–21, Mar. 2001.

[12] K. J. Binns and P. J. Lawrenson, *Analysis and Computation of Electric and Magnetic Field Problems: Pergamon International Library of Science, Technology, Engineering and Social Studies*, vol. 2, 2nd ed. Amsterdam, The Netherlands: Elsevier, 2013, ch. 2, pp. 16–21.

[13] P. E. Burke and T. H. Fawzi, "Effect of eddy losses on the design and modelling of air-cored reactors," *IEEE Trans. Magn.*, vol. 27, no. 6, pp. 5001–5003, Nov. 1991.

[14] S. Nogawa *et al.*, "Study of eddy-current loss reduction by slit in reactor core," *IEEE Trans. Magn.*, vol. 41, no. 5, pp. 2024–2027, May 2005.

[15] X. K. Yan, Z. B. Dai, C. Z. Yu, and Y. L. Qi, "Research on magnetic field and temperature field of air core power reactor," in *Proc. Int. Conf. Elect. Mach. Syst. (ICEMS)*, Beijing, China, Aug. 2011, pp. 1–4.

[16] C. D. A. Silveira, C. A. Da Costa, R. D. C. E. Silva, L. R. Soares, and J. C. P. Guimaraes, "Electromagnetic environment measurement under steady-state conditions in utility substations," in *Proc. IEEE/PES Transmiss. Distrib. Conf. Expo., Latin Amer.*, Caracas, Venezuela, Aug. 2006, pp. 1–6.

[17] G. Xu, L. Zou, L. Zhang, and T. Zhao, "Investigation on small-scale experiments of magnetic field around air-core reactors," *Appl. Mech. Mater.*, vol. 521, pp. 389–393, Feb. 2014.

[18] L. Zou, P. Gong, and L. Zhang, "Small-scale experiment and model simplification of space magnetic fields around air-core reactors," (in Chinese), *High Voltage Eng.*, vol. 40, no. 6, pp. 1675–1682, Jun. 2014.

[19] Q. Yu and S. A. Sebo, "Calculation accuracy of the planar filament current loop stack model of large air-core reactor coils," *IEEE Trans. Magn.*, vol. 33, no. 5, pp. 3313–3315, Sep. 1997.

[20] Q. Yu and S. A. Sebo, "Simplified magnetic field modeling and calculation of large air-core reactor coils," *IEEE Trans. Magn.*, vol. 32, no. 5, pp. 4281–4283, Sep. 1996.

[21] S. W. Du *et al.*, "Simplified calculation and coverage of power frequency magnetic field around 10 kV air-core reactors," (in Chinese), *High Voltage App.*, vol. 42, no. 3, pp. 179–182, Mar. 2006.

ZHIYUN HAN was born in Shuozhou, Shanxi, China, in 1995. He received the B.S. degrees from the School of Electrical Engineering, Shandong University, in 2016, where he is currently a Graduate Student. He is devoted to the research on the magnetic field distribution of dry-type air-core reactors.

LIANG ZOU received the B.Sc., M.Sc., and Ph.D. degrees from the School of Electrical Engineering, Shandong University, in 2004, 2007, and 2011, respectively. He is currently an Associate Professor and also a Master Supervisor with the School of Electrical Engineering, Shandong University. He is devoted to the research on the magnetization modeling theory of high-voltage electromagnetic equipment.

HAN SONG was born in Weifang, Shandong, China, in 1995. She received the B.S. degrees from the School of Electrical Engineering, Shandong University, in 2017, where she is currently a Graduate Student. She is devoted to the research on the magnetic field distribution of dry-type air-core reactors.

LI ZHANG received the B.Sc., M.Sc., and Ph.D. degrees from the School of Electrical Engineering, Shandong University, China, in 2001, 2005, and 2009, respectively. He is currently an Associate Professor with the School of Electrical Engineering, Shandong University, with a broad research interest covering power systems electromagnetic compatibility, condition monitoring, and reliability analysis of electrical equipment.

TONG ZHAO received the B.Sc. and Ph.D. degrees in electrical engineering from Shandong University, Jinan, China, in 2002 and 2008, respectively. He completed his Post-Doctoral Research in electrical engineering at Tsinghua University, China, from 2008 to 2010. He is currently an Associate Professor in electrical engineering with Shandong University. His special fields of interest include high-voltage engineering, condition monitoring, and fault diagnostics.

YOULIANG SUN received the B.Sc. degree in electrical engineering and electrical control from Hebei Technology University in 1997, and the M.Sc. degree in electrical engineering from North China Electric Power University in 2012. He is currently a professor-level Senior Engineer at the Shandong Electrical Engineering and Equipment Group Co., Ltd., Jinan, China. He is devoted to the research on UHV, converter transformers, and smoothing reactor of DC transmission.